APPLICATION OF BIG DATA ANALYSIS IN PATH PLANNING OF INTELLIGENT PICKING ROBOT

/

大数据分析在智能采摘机器人路径规划中的应用

Hejun Zhao[1) 2) *], Stoyanets Nataliya[1)], Guohou Li[3)]

[1)] Sumy National Agrarian University, Ukraine.

[2)] Xinxiang Vocational and Technical College, Xinxiang, Henan, China.

[3)] Henan Institute of Science and Technology, Henan, China.

**E-mail: ueooao@163.com*

Corresponding author: Dr. Hejun Zhao

DOI: https://doi.org/10.35633/inmateh-65-49

Keywords: *picking robot, path planning, big data analysis*

ABSTRACT

In order to solve the problem of autonomous movement of intelligent picking robot, a method for big data analysis is proposed. The data collected by laser ranging sensor, CCD camera and electronic compass are analyzed to determine the current robot position and heading. The robot walking route is preset in the orchard, and the nixie tube ground sign is installed. Because the coordinates of the ground sign are known, the heading angle of the robot can be determined by an electronic compass. The CCD camera captures the sign image, and adopts the methods of image graying, image segmentation, image corrosion and image thinning to extract the digital tube image data on the sign. Fuzzy control method is used to identify digital tube numbers on the ground sign, and CCD camera scans whether there are obstacles in front of the road at the same time. The laser ranging sensor completes two tasks: (1) detecting the sign distance and direction angle of the distance, and calculating the current position and heading angle of the robot through the coordinates of the sign; (2) detect the distance from obstacles, and start the obstacle avoidance system when it is less than 1m. The path planning system of picking robot based on big data analysis relies on a variety of sensors, and has a strong ability to perceive orchard environment, and it has high ability of path planning.

摘要

为了解决智能采摘机器人自主运动问题，一种面向大数据分析的方法被提出。对激光测距传感器、CCD 摄像机和电子罗盘等传感器采集的数据进行分析，确定当前机器人位置与航向。在果园中预先设定机器人行走路线，安装数码管地标牌。因为地标牌坐标已知，所以可用电子罗盘确定机器人航向角。CCD 摄像头拍摄地标牌图像，采用图像灰度化、图像分割、图像腐蚀及图像细化的方法提取表示牌上数码管图像数据。采用模糊控制方法识别地标牌上数码管数字，CCD 摄像头同时扫描行进前方是否有障碍物。激光测距传感器完成两个任务:①检测距离地标牌距离和方向角，通过标识牌坐标计算机器人当前位置与航向角;②检测与障碍物间距离，当小于 1m 时启动避障系统。基于大数据分析的采摘机器人路径规划系统依托多种传感器，对果园环境感知能力强，具有较高的路径规划能力。

INTRODUCTION

Path planning is one of the most important technologies in mobile robot navigation. Path planning means finding an optimal collision-free path from the starting point to the target point in a given environment with obstacles according to some performance indexes (such as shortest distance, shortest time or minimum energy consumption, etc.). For mobile robots, path planning optimization is to solve the problem of platform path optimization under specific working environment and task requirements. The scientific and rational path planning has a very important impact on the working efficiency of mobile robots *(Cerone A., 2019)*. At present, the commonly used path planning optimization methods can be divided into traditional algorithms and intelligent algorithms. Among them, traditional algorithms mainly include artificial potential field method, fuzzy logic algorithm, viewable method, grid method, free space method and so on. Since the path planning problem was put forward in 1970s, these traditional algorithms have played an important role in the field of robot path planning, and obtained many research results.

For example, in practical applications such as marine science, industrial field and military operations, these traditional path planning optimization methods have some defects when dealing with these complex environments *(Cheung K. S. et al., 2019)*. For example, the artificial potential field method is easy to fall into local minima, which has the problem that the target is unreachable, and the viewable method is inefficient and cannot meet the real-time requirements of path planning. Fuzzy control algorithm is difficult to establish fuzzy rule base in complex and changeable environment, and lacks intelligent obstacle avoidance strategy for dynamic obstacles *(Cza B. et al., 2021).*

In recent years, with the rise of artificial intelligence, more and more intelligent algorithms have been proposed and applied to the path planning optimization of mobile robots to overcome the limitations of traditional path planning algorithms. An important feature of these intelligent algorithms is that their operating mechanism is very similar to the biological group behavior or ecological mechanism in nature. Moreover, the efficiency of these intelligent algorithms is usually higher than that of traditional algorithms *(Fan T. et al., 2020)*. In order to distinguish them from traditional optimization algorithms, these intelligent algorithms are defined as intelligent bionic algorithms. CZA, B. think that fuzzy control is a control mode similar to human thinking ability, which has the reasoning ability and fuzziness of human intelligence. In the path planning of robot, fuzzy reasoning is often used, and the behaviors such as obstacle avoidance, speed regulation and target navigation of robots are generally referred to as robot movement *(Chen J. et al., 2005)*. *Garg et al,* believe that robots control these behaviors in different ways and choose the optimal traveling plan of robots through a series of decisions *(Garg H. et al., 2019)*. *Hasanipanah et al* thinks that besides fuzzy control methods, there are many algorithms for path planning, such as A-star algorithm, visibility method, artificial potential field method and ant colony algorithm *(Hasanipanah M. et al., 2020)*. In this system, walking track is preset for robot, landmark sign is made, and digital map with known coordinates of landmark sign is established. The robot adopts CCD camera, laser ranging sensor and electronic compass, and has strong environmental perception ability. Using big data fusion technology, multiple groups of signals are fused to determine the coordinate position and heading of the robot. CCD camera is used to identify road signs and obstacles, and laser ranging sensor is used to detect and identify road signs. The fuzzy control method is used to establish an obstacle avoidance system to judge the distance between the obstacle and the robot. Test results show that the system has high environmental awareness, and has good path planning performance *(Hou X., 2020)*.

MATERIALS AND METHODS

Sensors are the elements of a robot to obtain information, which can be called "eyes" of a mobile robot. Some basic behaviors of robots, such as positioning and navigation, environment modeling and avoiding obstacles, are realized through such eyes. The word data is in plural form as the input signal of the fuzzy controller by the sensor. Position sensing is an important condition for picking robot to work autonomously, and the robot senses its position in the digital map through sensors. This system uses multi-dimensional sensors to determine its own position, and cameras to photograph reference objects for terrain matching. The laser ranging sensor is adopted to detect the distance between itself and the reference object, and determine the head direction by electronic compass. The three groups of detected data are fused to finally determine the robot position *(Hu J. et al., 2019)*.

Robot Terrain Matching

Terrain matching system is used by robots to identify landmarks and indicate the direction of their next progress. Because the growth of fruit trees in apple orchards is similar, and the spacing is not much different, it is difficult to use each apple tree as a marker. According to the preset working track of the robot, eight-segment code numbers are written on white cardboard as position marks. Terrain matching mainly completes two tasks: (1) image processing, eliminating useless information of the image, and keeping only eight-segment digital images; (2) image recognition, determining the image number of eight-segment code *(Kumar P. B. et al., 2019)*. The image processing process includes: (1) image graying; (2) image segmentation; (3) image corrosion; (4) image thinning.

The process of converting a color image into a gray image becomes the gray processing of the image. The color of each pixel in the color image is determined by three components: R, G and B, and each component has 255 values. Such a pixel can have more than 16 million (255 * 255 * 255). The gray image is a special color image with the same R, G and B components, and the change range of one pixel is 255.

Therefore, in digital image processing, images of various formats are generally transformed into gray images to reduce the amount of calculation of subsequent images. The description of gray images is the same as that of color images However, it reflects the distribution and characteristics of the overall and local chromaticity and brightness levels of the whole image. Image segmentation is the technology and process of dividing an image into several specific regions with unique properties and putting forward the target of interest. It is a key step from image processing to image analysis. From a mathematical point of view, image segmentation is the process of dividing digital images into disjoint regions. The process of image segmentation is also a marking process, that is, pixels belonging to the same region are given the same number. The corrosion process of image is similar to the convolution operation of image. Template matrix is required to control the operation results. In the corrosion and expansion of image, this template matrix is called structural element, which is the same as convolution. Structural elements can arbitrarily specify the center point of image, and the volume content of structural elements can be defined according to their own needs. Image thinning generally refers to an operation of image skeletonization of binary images. Thinning is the abbreviation of the process of reducing image lines from multi-pixel width to unit pixel width. Some articles often describe the thinning results as "skeletonization", "middle axis conversion" and "symmetry axis conversion".

Now take the floor sign with the number "3" as an example to design. Because each pixel of each color picture is synthesized by RGB three-channel intensity, the amount of information is too complicated. Therefore, it can effectively reduce the amount of picture information by transforming color pictures into gray pictures by using the gray-scale method. When the image is segmented, the threshold k is calculated, and when the gray level of the picture pixel is greater than k, the point is assigned 255. When the gray level of a pixel is less than k, assign a value of 0 to the pixel to form a picture that is either black or white (as shown in Fig. 1). Etching the binary image, and a 3×3 reference matrix is established with a certain pixel as the center. When all pixels in the 3×3 reference matrix are 255, the value of this point is 255. On the contrary, assign a value of 0 to this point, and get the binary image of the ground sign showing the number "3". Image thinning is to peel off the image under the condition that the image connection is unchanged, and Hilditch thinning algorithm is selected to establish a 3×3 matrix of target pixels. After deleting this point, the number of connected domains remains unchanged, and then the median filtering method is used for noise reduction. Firstly, the 3×3 matrix of the target pixel point and the average gray levels (I_v) of 8 pixels around the point are calculated. When $|I_p - I_v| > 127.5$, I_p is 255. When $|I_p - I_v| < 127.5$, I_p is assigned to 0. The filtered image showing the number "3" sign is obtained *(Liu S. et al., 2020)*.

Fig. 1 - Landmark image processing

By extracting and compressing part of the image containing the nixie tube number, the pixel size of the image is 10 × 10 resolution. Establish a 10×10 constant matrix, scan the compressed image line by line, and assign a value of 1 to the corresponding constant matrix when the gray level of the pixel is 0; By analogy, the digital image information is extracted into a 10×10 constant matrix. In view of the fact that the signboard is composed of 10 digital tube numbers such as 0~9. The system needs to be able to identify 0~9. In the process of camera shooting, the recognition results will be affected by environmental light sources, weeds and leaves. Therefore, the BP neural network method is used for recognition to enhance the recognition accuracy and fault tolerance. The two most important indexes for establishing neural network are the number of hidden neurons and allowable error. The number of hidden neurons, namely the central value of membership function and the number of rule bases, determines the accuracy and complexity of the network. The allowable error is the error between the output and the expectation, which determines the number of calculation iterations.

The allowable error is the system acceptance value of the difference between the actual output and the expected output, which represents the approximation degree of the expected output of the actual output phase.

When the actual error is less than the allowable error, the neural network operation is finished, and the system outputs the recognition result. When the actual error is greater than the allowable error, the system performs the next iteration calculation until the allowable error is met. The influence of allowable error on the system is shown in Fig. 2. When the allowable error is 0.05, the training time is 920 Ms. With the increase of allowable error, the training time decreases gradually. When the allowable error is 0.05, the recognition accuracy is 87%. With the increase of the number of neurons in the hidden layer, the training time gradually increased and the training speed accelerated. However, the recognition rate increases at first and then decreases. When the number of neurons is 9, the recognition rate reaches the maximum. This is because the number of neurons increases, the complexity of the network increases, and the anti-noise ability decreases, resulting in a decrease in recognition rate *(Santos L. C. et al., 2021)*.

The allowable error is the system acceptance value of the difference between the actual output and the expected output, which represents the approximation degree of the expected output of the actual output phase. When the actual error is less than the allowable error, the neural network operation ends and the system outputs the recognition result. When the actual error is greater than the allowable error, the system performs the next iteration calculation until the allowable error is met. The influence of allowable error on the system is shown in Fig. 3. When the allowable error is 0.05, the training time is 920 ms. With the increase of allowable error, the training time decreases gradually. When the allowable error is 0.05, the recognition accuracy is 87%. At this time, the system recognizes that the number on the sign is "3". And then it gradually decreased. Considering the recognition rate and training time, the allowable error is 0.05. At this time, the system identifies the number on the sign of this place as "3" *(Tourajizadeh H. et al., 2020)*.

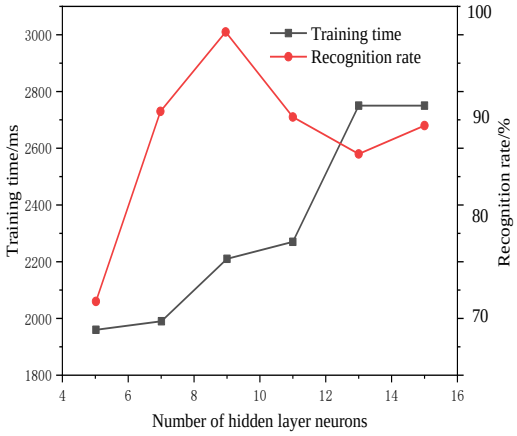

Fig. 2 - Influence of neuron number on neural network

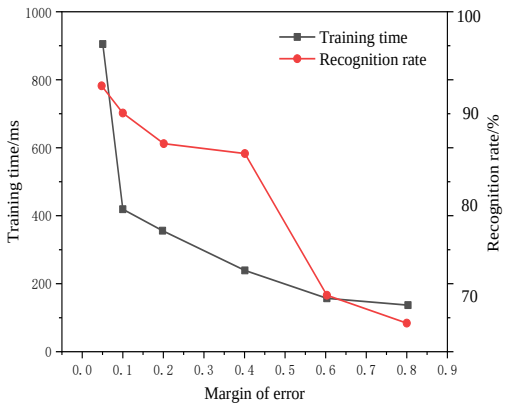

Fig. 3 - Error of allowable error to neural network

Calculation of Absolute Coordinates of Ground Signs

The detection of the coordinates of the ground sign includes two coordinate systems, as shown in Fig. 4. $(x_0,y_0)^T$, P_0 is the geometrical point, in fact after figure 4, $(X_0,Y_0)^T$. (Xo, Yo) are the absolute Cartesian coordinates in the plane of the reference point of the robot o, which must be specified, and (r,θ) are polar coordinates of the point P, in the local system of the robot, according to fig. 4. (X_P, Y_P) are the absolute Cartesian coordinates of the point P in the absolute reference system and (x_P, y_P) is the coordinates of the point P in the local reference system of the robot. The absolute coordinate system of P_0 is $P_0(x_0,y_0,\theta)^T$, and the coordinate of the target in the local coordinate system of the robot is $P_p(x_p,y_p)^T$. Because the distance of the marker is detected by the left and right radar ranging sensors in the local coordinate system of the robot, the detection data are distance r and azimuth α (between r and ox axis of robot moving axis system). Therefore, the local coordinates are expressed as:

$$\begin{aligned} x_p &= r\cos a \\ y_p &= r\sin a \end{aligned} \tag{1}$$

X_p is projected on x axis as $r\cos\alpha$, and y_p is projected on y axis as $r\sin\alpha$. Since the vector directions of the two are opposite, let the coordinate of P in the decision coordinate system be $P(x_g,y_g)^T$, then the abscissa x_g is:

$$x_g = x_p\cos\theta - y_p\sin\theta + x_0 \tag{2}$$

Y_g can be obtained in the same way.

$$y_g = x_p\sin\theta + y_p\cos\theta + y_0 \tag{3}$$

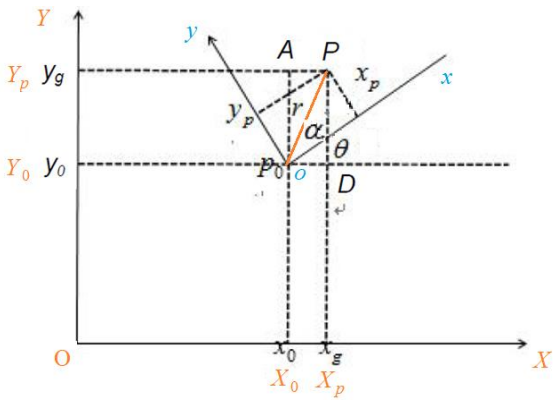

Fig. 4 - Coordinate transformation

Multi-Sensor Data Fusion

Use the electric compass to determine the current direction angle θ of the robot. Use cameras to identify landmarks and signs. The position coordinates (P) are known in the absolute coordinate system. The two laser distance sensors detect the distance r and the included Angle a between the robot and the position P of the ground sign, and the coordinates of the robot relative to the target in the coordinate system can be obtained. At present, it is necessary to calculate the robot's own position coordinates according to the above detection data. Since multiple sensors are used and the laser ranging sensors are divided into left and right ones, it is necessary to fuse multiple sets of detection data: (1) Fusion of the electric compass detection data and the ranging sensor data; (2) The left and right ranging sensors are fused, and finally the current robot position coordinates are deduced *(Wan S. et al., 2020)*.

Derive the position coordinates of the left ranging sensor from landmark coordinates. The relationship between the absolute coordinates of the landmark and the absolute coordinates of the position of the left ranging sensor can be obtained by formula (2) and formula (3), and the absolute position coordinate $P_{OL}(x_{OL},y_{OL})$ of the left sensor is:

$$\begin{bmatrix} x_{OL} \\ y_{OL} \end{bmatrix} = P_g - \begin{bmatrix} \cos\theta & -\sin\theta \\ \sin\theta & \cos\theta \end{bmatrix} \cdot \begin{bmatrix} x_{pL} \\ y_{pL} \end{bmatrix} \tag{4}$$

Similarly, the absolute position coordinate $P_{OR}(x_{OR},y_{OR})$ of the right sensor can be obtained as follows:

$$\begin{bmatrix} x_{OR} \\ y_{OR} \end{bmatrix} = P_g - \begin{bmatrix} \cos\theta & -\sin\theta \\ \sin\theta & \cos\theta \end{bmatrix} \cdot \begin{bmatrix} x_{pR} \\ y_{pR} \end{bmatrix} \quad (5)$$

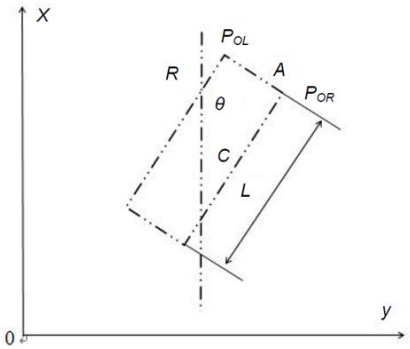

Fig. 5 - Robot coordinate calculation

The absolute coordinate $P_c(x_c,y_c)$ of robot center is shown in fig. 5. In fig. 5, it is necessary to fuse the coordinates of the left and right distance sensors, and calculate the coordinates of point a of the robot according to $P_{OR}(x_{OR},y_{OR})$ and $P_{OL}(x_{OL},y_{OL})$ coordinates, namely:

$$\begin{bmatrix} x_c \\ y_c \end{bmatrix} = \begin{bmatrix} \frac{x_{OR}+x_{OL}}{2} \\ \frac{y_{OR}+y_{OL}}{2} \end{bmatrix} \quad (6)$$

Vectors RA and CR are positive when they are in the same direction as the positive direction of coordinate axis and negative when they are opposite, then $RA=L\ sin\ \theta/2$, and $CR=L\ sin\ \theta/2$, then the absolute coordinates of the robot center P_C are:

$$\begin{bmatrix} x_c \\ y_c \end{bmatrix} = \begin{bmatrix} \frac{x_{OR}+x_{OL}}{2} - \frac{1}{2}L\sin\theta \\ \frac{y_{OR}+y_{OL}}{2} - \frac{1}{2}L\cos\theta \end{bmatrix} \quad (7)$$

RESULTS

Path planning is the whole process in which the robot travels from the starting point to the end according to the instructions of the target digital card. In the process of implementation, two problems are mainly solved, namely obstacle avoidance and target guidance. Finally, the unmanned traveling from the starting point to the end point is realized.

Obstacle Avoidance

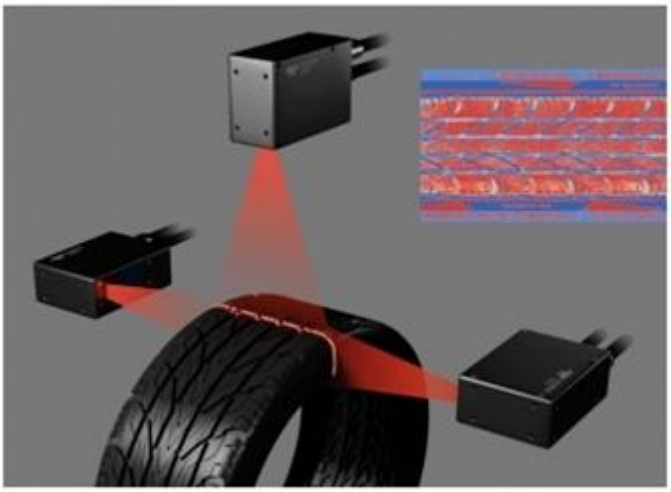

Fig. 6 - Image of 3D laser sensor

The schematic diagram of three-dimensional laser sensor is shown in Figure 6. It is difficult to give an exact concept of mobile robot obstacles in unknown environment. Intuitively, any object that forms a certain obstacle in the moving direction of the robot can become an obstacle. In recent years, the application of vision based obstacle recognition has attracted more and more attention. Obstacle avoidance uses two laser distance sensors as detection elements, and the detection data of the sensors are distance r and azimuth a. The minimum detection distance between the two sensors is r_{min}. When r_{min} is less than 1m, start the obstacle avoidance system. The obstacle avoidance system adopts fuzzy design. The input of the fuzzy system is the azimuth of two distance sensors, and the membership function has five central values, $-\pi/2$, $-\pi/4$, 0, $\pi/4$, $\pi/2$. When the left and right sensors detect obstacles are on the same side in the forward direction, the robot keeps its original direction unchanged. When the left and right sensors detect that the output of the membership function of the included angle of the obstacle is 0, the robot turns $\pi/2$ in the direction of smaller included angle; When that obstacle appear on both sides of the advance direction and are at the maximum and middle positions respectively, the robot turns $\pi/4$ to the maximum position. The obstacle avoidance planning is shown in Table 1 *(Zhou Y. et al., 2019)*.

Table 1

Obstacle avoidance rules

a_R	a_L				
	LB	LM	C	RM	RB
LB	C	C	RB	LM	C
LM	C	C	RB	C	RM
C	RB	RB	RB	LB	LB
RM	C	C	LB	JM	LM
RB	C	C	LB	LM	C

Target guidance

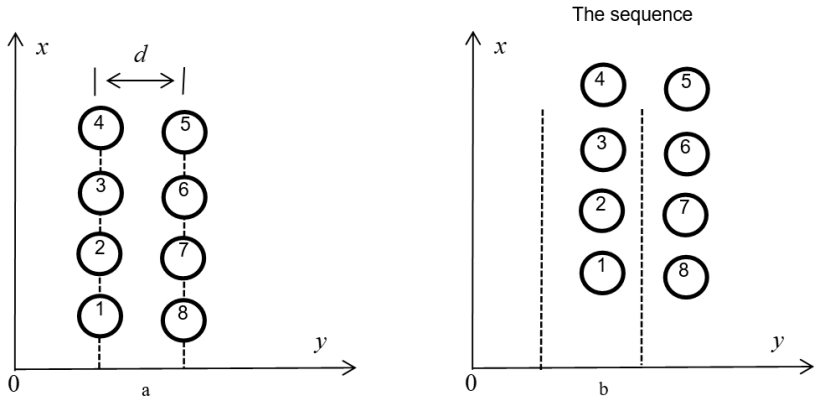

Fig. 7 - Target guidance

The robot is guided by the ground signs. Eight-segment codes such as 1, 2, 3, etc. are arranged on the planned travel route of the robot, and the distance between the two columns of trees is *d*. Since the signboard is installed on the tree, and the robot recognizes each signboard coordinate in the process of walking, the signboard coordinate shifts to the right by $d/2$ in the digital map system, as shown in fig. 7(a). The boot process is as follows:

1) The distance measuring sensor detects the coordinate $p(x,y)$ of the sign position and calculates the coordinate $p_c(x_c,y_c)$ of the robot, and the distance D between them is $D=\sqrt{(x-x_c)^2+(y-y_c)^2}$. 2) When $D>0.3$ m, the robot advances to the sign; when $D<0.3$ m, the robot stops and the camera starts looking for the next sign. 3) Determine whether the current signboard is the final target: if not, return to step 1); if yes, the robot stops moving, as shown in fig. 7(b).

System Test

The layout of the orchard referred to is similar to the plantation in Figure 8. In this case, it shall be specially arranged into an alley between rows of trees. The system test results are shown in Fig. 8.

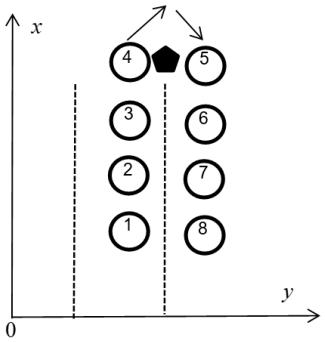

Fig. 8 - System test

Translate the coordinate of the sign to the right by $d/2$ to create a digital map. Starting from the "1" position, the robot first scans the camera to find the digital tube "2" and calculate the distance d. When $D>0.3$ m, the robot advances to the sign; When D<0.3 m, the robot stops. The camera starts looking for the next sign. When the robot moves to position "4", the robot position sensor scans and finds obstacles. When the distance from the obstacle is less than 1 m, the robot rotates $\pi/4$ counterclockwise and advances, then continues to scan the sign "5" and advances to the landmark 5, until it moves to the sign "8", when the system confirms that it has moved to the final target, and the robot stops moving. This topic is not described in detail. This paper does not develop this topic now, it should be used as the direction or goal of further research and development in the future. The schematic diagram of site acceptance test is shown in Figure 9.

Fig. 9 - Site acceptance test drawing

Since ancient times, mankind has been seeking inspiration for invention and creation from nature. It is found that individual behavior is very simple, but complex tasks can be completed through individual cooperation.

In these intelligent bionic algorithms, most of them are inspired by the foraging behavior of biological groups, such as ant colony algorithm, particle swarm algorithm, artificial fish swarm algorithm, bacterial foraging algorithm, Hybrid Shuffled Frog-Leaping Algorithm and artificial bee colony algorithm. Others are inspired by the behavior of other groups of organisms. The following mainly discusses the research results of some intelligent bionic algorithms inspired by the behavior of biological groups in the field of path planning and optimization of mobile robots. These field tests are done through a very laborious experimental activity. Good experimental results were obtained.

CONCLUSION

In order to realize the automatic walking of picking robot in orchard, big data fusion laser ranging sensor, CCD camera and electronic compass are used to collect data and calculate the current robot position coordinates and heading. When working, the left and right laser sensors mark the position of objects and obstacles. When the left and right laser sensors work, the obstacle position can be marked.

When the marking distance is less than 0.3m, the CCD camera starts scanning the next target. When the distance is less than 1m, the obstacle avoidance mechanism is activated. The system uses a variety of sensor data comprehensive analysis, has a strong orchard environment perception ability.

REFERENCES

[1] Cerone, A. (2019). Model mining: integrating data analytics, modelling and verification. *Journal of Intelligent Information Systems,* Vol. 52, Issue 3, pp. 501-532. United States;

[2] Chen J, Li L R. (2005) Path planning protocol for collaborative multi-robot systems, 2005 International Symposium on Computational Intelligence in Robotics and Automation. IEEE, pp. 721-726. Finland;

[3] Cheung K S., Leung W K., & Seto, W. K. (2019). Application of Big Data analysis in gastrointestinal research. World Journal of Gastroenterology, Vol. 25, Issue 24, pp. 2990-3008. China;

[4] Cza B., Pl A., Xl A., Mw, A., Wh C., Gang L. D., (2021). Application of compositional data analysis in geochemical exploration for concealed deposits: a case study of Ashele copper-zinc deposit, Xinjiang, China. *Applied Geochemistry,* Vol. 130, Issue 2, pp. 104997. England;

[5] Fan T., Liu Z., Ouyang J., Li P. (2020). Preparation of an intelligent oleophobic hydrogel and its application in the replacement of locally damaged oil pipelines. *ACS Applied Materials & Interfaces,* Vol. 12, Issue 46, pp. 52018-52027. United States;

[6] Garg H., Arora R. (2019). Generalized intuitionistic fuzzy soft power aggregation operator based on t-norm and their application in multicriteria decision-making. *International Journal of Intelligent Systems,* Vol. 34, Issue 2, pp. 215-246. United States;

[7] Hasanipanah M., Zhang W., Armaghani D. J., Rad, H. N. (2020). The potential application of a new intelligent based approach in predicting the tensile strength of rock. *IEEE Access*, Vol. 8, Issue 99, pp. 57148-57157. United States;

[8] Hou X. (2020). Haptic teleoperation of a multirotor aerial robot using path planning with human intention estimation. *Intelligent Service Robotics*, Issue 11, pp. 1-14. Germany;

[9] Hu J., Fang J., Du Y., Liu Z., Ji P. (2019). Application of PLS algorithm in discriminant analysis in multidimensional data mining. *Journal of supercomputing,* Vol. 75, Issue 9, pp. 6004-6020. United States;

[10] Kumar P. B., Rawat H., Parhi D. R. (2019). Path planning of humanoids based on artificial potential field method in unknown environments. *Expert Systems*, Vol. 36, Issue 2, pp. 1-12. England;

[11] Liu S., Liu S., Xiao H. (2020). Optimization of structural parameters of jet end in the underwater intelligent pigging robot. *Ocean Engineering*, Vol. 216, Issue 7, pp. 108092. England;

[12] Santos L. C., Santos A., Santos F. N., (2021), A Case Study on Improving the Software Dependability of a ROS Path Planner for Steep Slope Vineyards*. Robotics,* Vol. 10, Issue 3, pp. 103. United States;

[13] Tourajizadeh H., Gholami O., (2020), Optimal control and path planning of a 3PRS robot using indirect variation algorithm*. Robotica,* Vol. 38, Issue 5, pp. 903-924. England;

[14] Wan S., Lu J., Fan P., & Letaief K. B., (2020). Toward big data processing in IoT: path planning and resource management of UAV base stations in mobile-edge computing system. *IEEE Internet of Things Journal*, Vol.7, Issue 7, pp. 5995-6009. United States;

[15] Zhou Y., Li W., Yi P., & Guo Y. (2019). Behavioral ordered weighted averaging operator and the application in multiattribute decision making. *International Journal of Intelligent Systems,* Vol. 34, Issue 3, pp. 386-399. United States.